

UCSF

UC San Francisco Previously Published Works

Title

Clinical effect of white matter network disruption related to amyloid and small vessel disease

Permalink

<https://escholarship.org/uc/item/6jp7z2mv>

Journal

Neurology, 85(1)

ISSN

0028-3878

Authors

Kim, Hee Jin
Im, Kiho
Kwon, Hunki
et al.

Publication Date

2015-07-07

DOI

10.1212/wnl.0000000000001705

Peer reviewed

Clinical effect of white matter network disruption related to amyloid and small vessel disease

Hee Jin Kim, MD*
Kiho Im, PhD*
Hunki Kwon, MS
Jong-Min Lee, PhD
Changsoo Kim, MD,
PhD
Yeo Jin Kim, MD
Na-Yeon Jung, MD
Hanna Cho, MD
Byoung Seok Ye, MD
Young Noh, MD
Geon Ha Kim, MD
En-Da Ko
Jae Seung Kim, MD, PhD
Yeom Seong Choe, MD,
PhD
Kyung Han Lee, MD,
PhD
Sung Tae Kim, MD, PhD
Jae Hong Lee, MD, PhD
Michael Ewers, PhD
Michael W. Weiner, MD,
PhD
Duk L. Na, MD, PhD
Sang Won Seo, MD, PhD

Correspondence to
Dr. Seo:
sangwonseo@empal.com

Editorial, page 16

Supplemental data
at Neurology.org

ABSTRACT

Background: We tested our hypothesis that the white matter network might mediate the effect of amyloid and small vessel disease (SVD) on cortical thickness and/or cognition.

Methods: We prospectively recruited 232 patients with cognitive impairment. Amyloid was assessed using Pittsburgh compound B-PET. SVD was quantified as white matter hyperintensity volume and lacune number. The regional white matter network connectivity was measured as regional nodal efficiency by applying graph theoretical analysis to diffusion tensor imaging data. We measured cortical thickness and performed neuropsychological tests.

Results: SVD burden was associated with decreased nodal efficiency in the bilateral frontal, lateral temporal, lateral parietal, and occipital regions. Path analyses showed that the frontal nodal efficiency mediated the effect of SVD on the frontal atrophy and frontal-executive dysfunction. The temporoparietal nodal efficiency mediated the effect of SVD on the temporoparietal atrophy and memory dysfunction. However, Pittsburgh compound B retention ratio affected cortical atrophy and cognitive impairment without being mediated by nodal efficiency.

Conclusions: We suggest that a disrupted white matter network mediates the effect of SVD, but not amyloid, on specific patterns of cortical atrophy and/or cognitive impairment. Therefore, our findings provide insight to better understand how amyloid and SVD burden can give rise to brain atrophy or cognitive impairment in specific patterns. **Neurology® 2015;85:63–70**

GLOSSARY

AAL = automated anatomical labeling; **AD** = Alzheimer disease; **aMCI** = amnesic mild cognitive impairment; **DSM-IV** = *Diagnostic and Statistical Manual of Mental Disorders* (Fourth Edition); **DTI** = diffusion tensor imaging; **FLAIR** = fluid-attenuated inversion recovery; **MNI** = Montreal Neurological Institute; **PiB** = Pittsburgh compound B; **SVaD** = subcortical vascular dementia; **SVD** = small vessel disease; **svMCI** = subcortical vascular mild cognitive impairment; **WM** = white matter; **WMH** = white matter hyperintensity.

Alzheimer disease (AD) is characterized by accumulation of β -amyloid plaques and temporoparietal atrophy, resulting in memory dysfunction.^{1,2} Subcortical vascular dementia (SVaD) is typically identified by extensive small vessel disease (SVD) markers and frontal atrophy, resulting in frontal-executive dysfunction.³ However, it remains unknown how atrophy in specific regions or cognitive impairment in specific domains arises from amyloid and SVD burden, the 2 most commonly coexisting pathologies in patients with dementia.^{4,5}

Graph theoretical analysis using diffusion tensor imaging (DTI) data can facilitate examination of large-scale white matter (WM) connectivity of the human brain from a network perspective.⁶ There is increasing evidence that patients with AD and SVD demonstrate a disrupted WM network.^{7–9}

*These authors contributed equally to this work.

From the Departments of Neurology (H.J.K., Y.J.K., N.-Y.J., E.-D.K., D.L.N., S.W.S.), Nuclear Medicine (Y.S.C., K.H.L.), and Radiology (S.T.K.), Samsung Medical Center, Sungkyunkwan University School of Medicine, Seoul; Neuroscience Center (H.J.K., Y.J.K., N.-Y.J., E.-D.K., D.L.N., S.W.S.), Samsung Medical Center, Seoul, Korea; Division of Newborn Medicine (K.I.), Boston Children's Hospital, Harvard Medical School, Boston, MA; Department of Biomedical Engineering (H.K., J.-M.L.), Hanyang University, Seoul, Korea; Division of Preventive Medicine (C.K.), Department of Medicine, Brigham and Women's Hospital and Harvard Medical School, Boston, MA; Departments of Preventive Medicine (C.K.) and Neurology (B.S.Y.), and Department of Neurology, Gangnam Severance Hospital (H.C.), Yonsei University College of Medicine, Seoul; Department of Neurology (Y.N.), Gachon University Gil Medical Center, Incheon; Ewha Womans University Mokdong Hospital (G.H.K.), Ewha Womans University School of Medicine, Seoul; Departments of Nuclear Medicine (J.S.K.) and Neurology (J.H.L.), University of Ulsan College of Medicine, Asan Medical Center, Seoul, Korea; Institute for Stroke and Dementia Research (M.E.), Ludwig-Maximilians-University, Munich, Germany; and Center for Imaging of Neurodegenerative Diseases (M.W.W.), University of California, San Francisco; Department of Clinical Research Design and Evaluation (D.L.N., S.W.S.), SAHST, Sungkyunkwan University, Seoul, Korea.

Go to Neurology.org for full disclosures. Funding information and disclosures deemed relevant by the authors, if any, are provided at the end of the article.

However, the clinical effect of WM network disruption related to amyloid and SVD remains unknown. With the following evidence, we suggest that the WM network might be a key link between amyloid/SVD burden and cortical atrophy or cognitive impairment: (1) alteration in the WM network was associated with cognitive impairment,¹⁰ (2) propagation of amyloid fibrils and progression of brain atrophy occurred along WM fiber pathways,¹¹ and (3) the topography of cortical atrophy related to WM hyperintensity (WMH) was similar to cortical regions connected via WM tracts, suggesting that cortical regions that are interconnected via the damaged tracts might become atrophic.¹²

We tested the hypothesis that the WM network might be a key link between amyloid/SVD burden and cortical atrophy or cognitive impairment. We then performed path analyses to evaluate whether the WM network mediates the association between amyloid/SVD burden and cortical atrophy or cognition.

METHODS Participants. We prospectively recruited 251 participants with cognitive impairment who underwent Pittsburgh compound B (PiB)-PET and structural brain MRI, from July 2007 to July 2011. All participants were clinically diagnosed at Samsung Medical Center. Patients with amnesic mild cognitive impairment (aMCI, $n = 45$) and those with subcortical vascular mild cognitive impairment (svMCI, $n = 67$) met the Petersen criteria for mild cognitive impairment with modifications.¹³ Patients with probable AD dementia ($n = 69$) met criteria proposed by the National Institute of Neurological and Communicative Disorders and Stroke and the Alzheimer's Disease and Related Disorders Association.¹⁴ Patients with SVaD ($n = 70$) met the diagnostic criteria for vascular dementia as determined by the *DSM-IV*, and also met the imaging criteria for SVaD proposed by Erkinjuntti et al.¹⁵ Patients with svMCI and SVaD had severe WMH on fluid-attenuated inversion recovery (FLAIR) images, which was defined as periventricular WMH ≥ 10 mm and deep WMH ≥ 25 mm, as modified from the Fazekas ischemia criteria.¹⁶ Patients with aMCI and AD were classified as having minimal (periventricular WMH < 5 mm and deep WMH < 5 mm) or moderate WMH (between minimal and severe WMH). The WMH meets the definition of WMH of presumed vascular origin, recently proposed by Wardlaw et al.¹⁷

Patients with territorial infarctions, WMH due to radiation injury, leukodystrophy, multiple sclerosis, or vasculitis were excluded. All patients underwent a clinical interview and neurologic examination. In addition, complete blood count, blood chemistry, vitamin B₁₂/folate level, syphilis serology, thyroid function, and *APOE* genotype were tested through blood sample.

Standard protocol approvals, registrations, and patient consents. This study was approved by the institutional review board of Samsung Medical Center. We obtained written consent from each patient.

PiB-PET acquisition and data analysis. All patients completed an [¹¹C]PiB-PET scan at Samsung Medical Center or Asan

Medical Center. All participants completed the same type of PET scan with a Discovery STe PET/CT scanner (GE Medical Systems, Milwaukee, WI). When measuring PiB retention, cerebellar gray matter was used as the reference region. We defined the PiB retention ratio as a continuous variable representing amyloid burden. The detailed radiochemistry profiles, scanning protocol, and PiB-PET data analysis are described in appendix e-1 on the *Neurology*[®] Web site at Neurology.org and in a previous study.⁵

MRI techniques. We acquired standardized T2, 3-dimensional T1 turbo field echo, 3-dimensional FLAIR, and DTIs from all participants at Samsung Medical Center using the same 3.0T MRI scanner (Philips 3.0T Achieva; Philips Healthcare, Andover, MA). Detailed imaging parameters are described in appendix e-2. In whole-brain DTI-MRI examination, sets of axial diffusion-weighted single-shot echo-planar images were collected with the following parameters: 128×128 acquisition matrix; $1.72 \times 1.72 \times 2$ mm³ voxel size; 70 axial slices; 22×22 cm² field of view; echo time 60 milliseconds, repetition time 7,696 milliseconds; flip angle 90°; slice gap 0 mm; b-factor of 600 s/mm². Diffusion-weighted images were acquired from 45 different directions using the baseline image without weighting (0, 0, 0). All axial sections were acquired parallel to the anterior commissure–posterior commissure line.

Measurement of WMH volume and lacunes. We measured volume of WMH (in milliliters) on FLAIR images using an automated method.¹⁸ Detailed methods are described in appendix e-3.

A lacune was defined as a lesion ≥ 3 mm and ≤ 15 mm in diameter with low signal on T1-weighted images, high signal on T2-weighted images, and perilesional halo on FLAIR images. This meets the definition of lacune of presumed vascular origin, recently proposed by Wardlaw et al.¹⁷ Two neurologists manually counted the number of lacunes, with a κ value of 0.78.

Network node definition. We used the automated anatomical labeling (AAL) atlas¹⁹ to parcellate the entire cerebral cortex into 78 areas (39 regions in each hemisphere) and to define the nodes of a brain graph. Individual T1-weighted images were nonlinearly registered to the ICBM152 T1 template in Montreal Neurological Institute (MNI) space.²⁰ The AAL atlas was transformed from MNI space to T1 native space using the inverse transformation with a nearest-neighbor interpolation method.

Network edge definition. We corrected distortions in DTIs caused by eddy currents and simple head motions by using the diffusion toolbox of the FSL (FMRIB's Software Library) package (www.fmrib.ox.ac.uk/fsl/fdt). Diffusion tensor models were estimated, and fractional anisotropy and mean diffusivity were calculated at each voxel. Whole-brain WM fiber tracts in native diffusion space for each participant were reconstructed using fiber assignment by a continuous tracking algorithm²¹ that is embedded in the Diffusion Toolkit (trackvis.org).²² Tracking was terminated when the angle between 2 consecutive orientation vectors was greater than 45°, or when both ends of the fibers extended outside of the WM mask that was generated by the tissue segmentation process.^{23,24} A fiber cutoff filter was applied so that fibers shorter than 20 mm and longer than 200 mm were filtered.

Using the affine registration tool from the FSL package (www.fmrib.ox.ac.uk/fsl/flirt), we coregistered T1-weighted images to the b0 images. Reconstructed whole-brain fiber tracts were inversely transformed into T1 space and fiber tracts and AAL-based parcellated regions were located in the same space. We assume that 2 nodes (regions) were structurally connected by an edge when at least the end points of 3 fiber tracts were located in these 2 regions. We selected a threshold number of fiber tracts to reduce the risk of false-positive connections due to noise or limitations of deterministic tractography.^{24,25} In this study, a mean fractional anisotropy

value along all the fibers connecting a pair of regions was used to weight the edge. Finally, weighted WM networks represented by symmetric 78×78 matrices were constructed for each individual.

Network analysis. Graph theoretical analyses were performed on weighted connectivity networks using the Brain Connectivity Toolbox (www.brain-connectivity-toolbox.net).²⁶ We used *nodal efficiency* as a nodal topological characteristic. Nodal efficiency is defined using the inverse of the weighted shortest path length between a given node and all other nodes in the network.²⁶ This metric quantifies the importance of nodes for communication within the network. Nodal efficiency was measured for each node, and averaged values of the nodal efficiency (mean nodal efficiency) in the frontal and temporoparietal regions predefined in the AAL atlas were used for global analysis.

Of 251 participants, we excluded 6 patients for whom WMH volume measurement failed because of segmentation errors, and 13 for whom the quality of diffusion image (low signal-to-noise ratio) was not sufficient to reconstruct reliable fiber tracts. Thus, network analysis was performed in 232 participants.

Cortical thickness data analysis. T1-weighted images were processed using the standard MNI anatomical pipeline. Further image processing for cortical thickness measurements is described in appendix e-4. In this way, we obtained the mean thickness of the frontal lobe and temporoparietal lobe.

Neuropsychological tests. Participants underwent neuropsychological tests using a standardized neuropsychological battery.²⁷ Based on the neuropsychological results, we calculated memory and frontal-executive subdomain scores.²⁸ Memory-domain score (memory score) was calculated by summing scores in orientation,

verbal memory, and visual memory tests. The memory score ranged from 0 to 150. Frontal-executive-domain score (executive score) was calculated by summing scores in a category word generation task, a phonemic word generation task, and the Stroop color reading test. The executive score ranged from 0 to 55.

Because of missing data in the memory score ($n = 10$) and executive score ($n = 21$), path analysis for the memory score was performed with data from 222 patients, and path analysis for the executive score was performed with data from 211 patients.

Statistical analysis. To evaluate the association between neuroimaging markers (PiB retention ratio, WMH volume, lacune number) and nodal efficiency, multiple linear regression analysis was performed for each node. We entered age, sex, education, PiB retention ratio, WMH volume, and lacune number to find the independent effects of each imaging marker. False discovery rate correction was performed to correct for multiple comparisons in 78 node regions.

To evaluate whether alteration of the WM network mediates the effects of SVD markers and amyloid burden on cortical thickness and cognition, path analyses were performed after controlling for age, sex, and education. Path analysis was used to simultaneously consider the direct, indirect, and total effects of predictors on outcomes through mediators. Because our intention was to focus on frontal-executive and memory function, we selected nodes or cortical regions that were related to frontal-executive function (bilateral frontal lobe) when evaluating frontal-executive function, and selected nodes or cortical regions that were related to memory (bilateral temporal and parietal lobe) when evaluating memory function (appendix e-5). Path analysis using executive score as the outcome was performed using mean

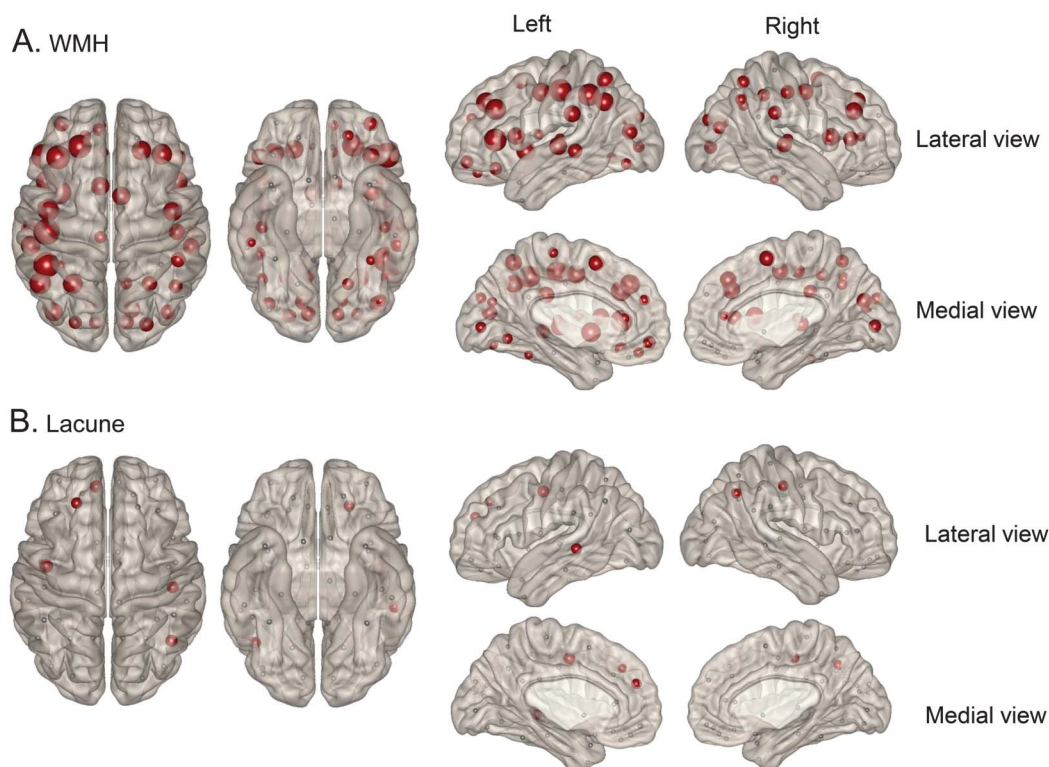
Table 1 Demographics of participants

	Total	aMCI	AD	svMCI	SVaD
No.	232	43	64	59	66
Demographics					
Age, y	72.1 (8.1)	70.1 (7.9)	69.7 (9.5)	74.1 (6.6)	73.7 (7.2)
Sex, female, n (%)	131 (56.5)	20 (46.5)	40 (62.5)	34 (57.6)	37 (56.1)
Education, y	10.1 (5.4)	12.4 (4.7)	10.4 (5.7)	9.8 (5.4)	8.7 (5.1)
Cardiovascular risk factors, n (%)					
Hypertension	144 (62.1)	16 (37.2)	34 (53.1)	43 (72.9)	51 (77.3)
Diabetes mellitus	47 (20.3)	5 (11.6)	10 (15.6)	16 (27.1)	16 (24.2)
Hyperlipidemia	68 (29.3)	10 (23.3)	15 (23.4)	18 (30.5)	25 (37.9)
Heart disease	34 (14.7)	7 (16.3)	5 (7.8)	16 (27.1)	6 (9.1)
APOE genotype, n (%)^a					
ε2 allele carrier	18/225 (8.0)	3/41 (7.3)	3/62 (4.8)	7/59 (11.9)	5/63 (7.9)
ε4 allele carrier	82/225 (36.4)	16/41 (39.0)	33/62 (53.2)	14/59 (23.7)	19/63 (30.2)
Small vessel MRI markers					
WMH volume, mL	22.9 (22.3)	3.2 (3.2)	5.1 (6.7)	33.8 (17.9)	43.2 (18.5)
Lacunae, n	6.7 (12.1)	0.6 (2.2)	0.3 (0.8)	7.5 (8.5)	16.4 (17.0)
Global PiB retention ratio	1.8 (0.5)	1.8 (0.5)	2.2 (0.4)	1.5 (0.4)	1.6 (0.5)
MMSE score	22.4 (5.7)	25.4 (4.7)	18.5 (5.8)	26.4 (2.8)	20.6 (4.9)

Abbreviations: AD = Alzheimer disease; aMCI = amnesic mild cognitive impairment; MMSE = Mini-Mental State Examination; PiB = Pittsburgh compound B; SVaD = subcortical vascular dementia; svMCI = subcortical vascular mild cognitive impairment; WMH = white matter hyperintensities. Values are expressed as mean (SD) or n (%).

^aAPOE genotyping was performed in 225 of 232 participants.

Figure 1 Topography of nodal efficiency related to WMH (A) and lacunes (B)



Statistically significant nodes are colored in red (false discovery rate-corrected $p < 0.05$). The size of the node sphere represents a standardized regression coefficient. WMH = white matter hyperintensities.

frontal nodal efficiency and mean frontal thickness as mediators (path analysis A). Path analysis using memory score as the outcome was performed using mean temporoparietal nodal efficiency and mean temporoparietal thickness as mediators (path analysis B). The pathobiological model of complex relationships between various factors is shown in figure e-1. We also performed subgroup analyses in patients with aMCI and AD (appendix e-6, table e-1, figure e-2). Amos version 18.0 software (SPSS, Chicago, IL) was used for all path analyses using maximum likelihood estimation.

RESULTS Demographics. The characteristics of our study participants are shown in table 1.

Decreased regional nodal efficiency related to SVD or amyloid burden. Increased WMH volume was associated with decreased nodal efficiency in the bilateral frontal, lateral temporal, lateral parietal, and occipital regions sparing the medial temporal and precuneus regions (figure 1A, table e-2). Increased number of lacunes was associated with decreased nodal efficiency in the left frontal, lateral temporal, and right lateral parietal regions (figure 1B, table e-2). There were no regions where PiB retention ratio was associated with decreased nodal efficiency.

Path analyses. Prediction of frontal-executive function and frontal cortical thickness. The path analysis for executive score showed goodness of fit to the data: $\chi^2 = 14.65$, degrees of freedom = 9, $p = 0.101$, comparative

fit index = 0.986, and root-mean-square error of approximation = 0.055 (table 2, figure 2A). Increased WMH volume and lacunes were associated with decreased mean frontal nodal efficiency, which was further associated with decreased mean frontal thickness that led to decreased executive score. Decreased mean frontal nodal efficiency was associated with decreased executive score without being mediated by frontal thickness. Increased number of lacunes was associated with decreased executive score without being mediated by frontal nodal efficiency or thickness. Increased PiB retention ratio was associated with decreased executive score without being mediated by frontal nodal efficiency.

Prediction of memory function and temporoparietal cortical thickness. The path analysis for memory score showed goodness of fit to the data: $\chi^2 = 13.93$, degrees of freedom = 10, $p = 0.176$, comparative fit index = 0.991, and root-mean-square error of approximation = 0.042 (table 2, figure 2B). Increased WMH volume and lacunes were associated with decreased mean temporoparietal nodal efficiency, which in turn was associated with decreased mean temporoparietal thickness, which led to decreased memory score. In contrast to WMH or lacunes, PiB retention ratio affected memory score without being mediated by nodal efficiency. Increased PiB retention ratio was associated with

Table 2 Effects of predictors (WMH volume, number of lacunes, and PiB retention ratio) on frontal-executive and memory function through mediators (mean nodal efficiency and mean cortical thickness)

	Path analysis A								
	Mean frontal nodal efficiency			Mean frontal thickness			Executive score		
	β	SE	p Value	β	SE	p Value	β	SE	p Value
WMH volume, mL	-0.374	0.073	0.010	-0.206	0.102	0.074	0.024	0.075	0.676
Lacunes, n	-0.206	0.068	0.015	0.074	0.076	0.405	-0.188	0.064	0.024
Global PiB retention ratio	0.076	0.059	0.224	-0.080	0.061	0.231	-0.244	0.062	0.010
Mean frontal nodal efficiency				0.424	0.08	0.010	0.223	0.071	0.010
Mean frontal thickness							0.288	0.065	0.010
	Path analysis B								
	Mean temporoparietal nodal efficiency			Mean temporoparietal thickness			Memory score		
	β	SE	p Value	β	SE	p Value	β	SE	p Value
WMH volume, mL	-0.359	0.057	0.010	-0.190	0.082	0.036	0.141	0.067	0.065
Lacunes, n	-0.237	0.065	0.010	0.044	0.078	0.565	-0.149	0.074	0.087
Global PiB retention ratio	0.031	0.061	0.669	-0.230	0.067	0.010	-0.420	0.052	0.010
Mean temporoparietal nodal efficiency				0.326	0.067	0.010	0.044	0.087	0.661
Mean temporoparietal thickness							0.350	0.056	0.010

Abbreviations: β = standardized beta coefficient; PiB = Pittsburgh compound B; SE = standard error; WMH = white matter hyperintensities. Values shown are the results of path analyses for executive score (path analysis A) and memory score (path analysis B).

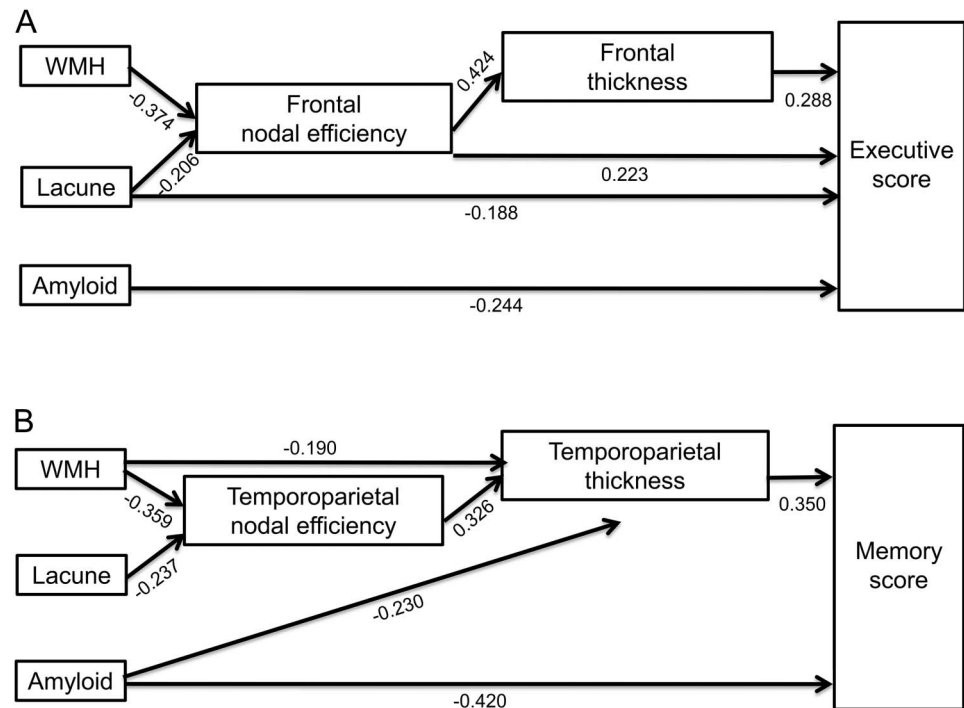
decreased mean temporoparietal thickness, which in turn was associated with decreased memory score. Increased PiB retention ratio was also associated with decreased memory score without being mediated by temporoparietal nodal efficiency or thickness.

We also investigated these relationships using nodal strength, which is another local measure. The results were generally similar to those of nodal efficiency (figures e-3 and e-4, table e-3).

DISCUSSION The present study examined the clinical effect of WM network disruption related to amyloid and SVD burdens. Our major findings were as follows: (1) SVD burden was associated with decreased nodal efficiency in widespread regions sparing medial temporal and precuneus regions, while there were no regions where amyloid burden was related to nodal efficiency; (2) SVD burden resulted in frontal or temporoparietal atrophy and frontal-executive or memory dysfunction via disruption of the corresponding WM network; and (3) amyloid burden affected cortical atrophy and cognitive impairment without being mediated by the WM network. Taken together, our findings suggest that alteration of the WM network mediates the effects of SVD burden on cortical atrophy and/or cognitive impairment. Furthermore, our findings provide insight to better understand how amyloid and SVD burden can give rise to brain atrophy in specific patterns or cognitive impairment in specific domains.

Our first major finding was that WMH were associated with decreased nodal efficiency in widespread regions. Several studies have already shown relationships between SVD markers and WM injury.^{29,30} However, to our knowledge, only a few studies have evaluated these relationships from a regional network perspective.⁸ Nodal efficiency, one of the network parameters, quantifies the importance of each node for communication within a network. As expected, WMH mostly affected nodal efficiency in the frontal regions. This is consistent with a previous study, which showed that WMH were associated with frontal hypometabolism or frontal-executive dysfunction regardless of their locations.³¹ In addition to the frontal regions, larger WMH volume was associated with decreased nodal efficiency in the lateral temporal and lateral parietal regions. This is supported by a recent study showing that WMH were associated with memory, language, and visuospatial dysfunctions as well as frontal-executive dysfunction.³² Of note, the topography of decreased nodal efficiency related to WMH relatively spared the medial temporal or precuneus regions. Previous studies have shown that the precuneus is a major hub region in the brain³³ and is involved in the early stage of AD.^{34,35} However, the current results might be supported by our previous study, which showed that patients with svMCI or SvAD who had profound WMH, but no significant amyloid burdens, had the entire cortical atrophy with

Figure 2 Schematic diagram of the path analyses for executive (A) and memory score (B)



White matter hyperintensity (WMH) volume, lacune number, and amyloid burden were entered as predictors. Mean nodal efficiency and mean cortical thickness in specific regions were entered as mediators. Age, sex, and education were entered as covariates. Numbers on the paths are standardized coefficients that were statistically significant.

the exception of the precuneus.³⁶ Furthermore, regions of decreased nodal efficiency related to WMH overlapped with regions of cortical atrophy related to WMH.¹² Therefore, it is conceivable that disruption of the WM network by WMH might be related to the development of cortical atrophy. Moreover, sparing of precuneus might be a feature discriminating patients with pure svMCI or pure SVaD from those with AD pathologies.

We found that the regional effects of lacunes on nodal efficiency were less widespread than those of WMH. This might be explained by differences in the regional involvement of the 2 SVD markers. That is, most lacunes occur focally in subcortical gray matter, while WMH usually involve widespread WM regions that contain long projection and association fasciculi connecting various cortical regions.³⁷

Our second major finding was that SVD burden was associated with frontal/temporoparietal atrophy and frontal-executive/memory dysfunctions via disruption of the corresponding WM network. We have noted that decreased nodal efficiency and cortical atrophy regions related to WMH are similar; this indicates that the disrupted WM network might be a key link between SVD burden and cortical atrophy. That is, cerebral hypoperfusion induced by SVD leads to ischemia in WM regions, causing demyelination and axonal loss of the WM network, which in turn results in

secondary damage to neuronal cell bodies and gray matter atrophy. It is generally accepted that when brain axons are injured, degeneration of the neuron occurs both proximally (dying back) and distally (Wallerian degeneration).^{38,39} Therefore, our findings suggest that SVD burden affects the WM network in the frontal and temporoparietal regions, resulting in corresponding cortical atrophy and eventually cognitive dysfunction. Alternatively, it is also possible that an ischemic process that affects gray matter and causes loss of neuronal cell bodies that have high metabolic demands leads to axonal degeneration, measured as WM network disruption and WMH. The sequential order and cause-effect relationships between gray matter loss and WM damage need to be investigated with longitudinal studies.

We also found that the disrupted frontal WM network affected frontal-executive dysfunction without mediating frontal atrophy. We previously reported that WMH independently affected cognitive impairment regardless of cortical atrophy.¹² Our findings are in line with a recent study that showed that disturbances in WM connectivity explained a substantial proportion of the variance in cognitive function on top of markers of brain atrophy.¹⁰ Furthermore, we found that lacunes affected frontal-executive dysfunction without mediating the WM network or causing cortical atrophy in the frontal lobe.

In contrast to SVD burden, amyloid burden affected cognitive impairment without mediating the structural WM network. This trend was observed when we performed path analyses for both memory score and executive score. Although a previous study suggested that patients with AD had a disrupted WM network,⁹ the amyloid burden was not quantified, thus the results may have been derived from combined WM lesions. Our findings suggest that the WM network might be unaffected by amyloid when the SVD burden is thoroughly controlled.

There are several limitations to our study. First, we used a single diffusion tensor–based deterministic tractography algorithm, which does not detect fiber crossings. For future studies, advanced high angular resolution diffusion imaging methods⁴⁰ should be used. Second, because of the cross-sectional nature of the study, we could only suggest associations. Further longitudinal studies are needed. Third, PiB-PET may not be sufficiently sensitive to detect soluble amyloid oligomers, diffuse amyloid plaques, or neurofibrillary tangle-predominant AD. Fourth, brain nodes related to frontal-executive or memory functions are widely distributed and parcellating functional areas based on an anatomical atlas may create some bias. Finally, our path analyses did not unravel their direct causative sequence. Nevertheless, our findings have implications for understanding how abnormalities in WM connectivity underlie the relationship between amyloid/SVD burden and cognition.

AUTHOR CONTRIBUTIONS

Dr. Sang Won Seo had full access to all of the data in the study and takes responsibility for the integrity of the data and the accuracy of the data analysis. Study concept and design: Hee Jin Kim, Kiho Im, Jong-Min Lee, and Sang Won Seo. Acquisition, analysis, or interpretation of data: Na-Yeon Jung, Yeo Jin Kim, Changsoo Kim, Hanna Cho, Byoung Seok Ye, Young Noh, Geon Ha Kim, En-Da Ko, Yearn Seong Choe, Kyung Han Lee, Sung Tae Kim, Jae Seung Kim. Critical revision of the manuscript for important intellectual content: Jae Hong Lee, Michael Ewers, Michael W. Weiner, Duk L. Na. Drafting of the manuscript: Sang Won Seo and Hee Jin Kim.

STUDY FUNDING

This study was supported by the Basic Research Program through the National Research Foundation of Korea (NRF) funded by the Ministry of Education (NRF-2013R1A1A2065365), by the Korean Healthcare Technology R&D Project Ministry for Health & Welfare Affairs (HI10C2020 & HIC120713), by the Korea Ministry of Environment (MOE) as the Environmental Health Action Program (2014001360002), by the KOSEF NRL program grant (MEST; 2011-0028333), by Samsung Medical Center (CRL-108011 & CRS110-14-1), and by the Converging Research Center Program through the Ministry of Science, ICT and Future Planning, Korea (2013K000338).

DISCLOSURE

The authors report no disclosures relevant to the manuscript. Go to Neurology.org for full disclosures.

Received September 23, 2014. Accepted in final form February 5, 2015.

REFERENCES

1. Braak H, Braak E. Neuropathological staging of Alzheimer-related changes. *Acta Neuropathol* 1991;82:239–259.

2. Jack CR, Knopman DS, Jagust WJ, et al. Hypothetical model of dynamic biomarkers of the Alzheimer's pathological cascade. *Lancet Neurol* 2010;9:119–128.
3. Roman GC, Erkinjuntti T, Wallin A, Pantoni L, Chui HC. Subcortical ischaemic vascular dementia. *Lancet Neurol* 2002;1:426–436.
4. Schneider JA, Arvanitakis Z, Bang W, Bennett DA. Mixed brain pathologies account for most dementia cases in community-dwelling older persons. *Neurology* 2007;69:2197–2204.
5. Lee JH, Kim SH, Kim GH, et al. Identification of pure subcortical vascular dementia using 11C-Pittsburgh compound B. *Neurology* 2011;77:18–25.
6. Sporns O, Tononi G, Kotter R. The human connectome: a structural description of the human brain. *PLoS Comput Biol* 2005;1:e42.
7. He Y, Chen Z, Evans A. Structural insights into aberrant topological patterns of large-scale cortical networks in Alzheimer's disease. *J Neurosci* 2008;28:4756–4766.
8. Lawrence AJ, Chung AW, Morris RG, Markus HS, Barrick TR. Structural network efficiency is associated with cognitive impairment in small-vessel disease. *Neurology* 2014;83:304–311.
9. Lo CY, Wang PN, Chou KH, Wang J, He Y, Lin CP. Diffusion tensor tractography reveals abnormal topological organization in structural cortical networks in Alzheimer's disease. *J Neurosci* 2010;30:16876–16885.
10. Reijmer YD, Leemans A, Caeyenberghs K, et al. Disruption of cerebral networks and cognitive impairment in Alzheimer disease. *Neurology* 2013;80:1370–1377.
11. Raj A, Kuceyeski A, Weiner M. A network diffusion model of disease progression in dementia. *Neuron* 2012;73:1204–1215.
12. Seo SW, Lee JM, Im K, et al. Cortical thinning related to periventricular and deep white matter hyperintensities. *Neurobiol Aging* 2012;33:1156–1167.
13. Seo SW, Cho SS, Park A, Chin J, Na DL. Subcortical vascular versus amnesic mild cognitive impairment: comparison of cerebral glucose metabolism. *J Neuroimaging* 2009;19:213–219.
14. McKhann G, Drachman D, Folstein M, Katzman R, Price D, Stadlan EM. Clinical diagnosis of Alzheimer's disease: report of the NINCDS-ADRDA Work Group under the auspices of Department of Health and Human Services Task Force on Alzheimer's Disease. *Neurology* 1984;34:939–944.
15. Erkinjuntti T, Inzitari D, Pantoni L, et al. Research criteria for subcortical vascular dementia in clinical trials. *J Neural Transm Suppl* 2000;59:23–30.
16. Fazekas F, Kleinert R, Offenbacher H, et al. Pathologic correlates of incidental MRI white matter signal hyperintensities. *Neurology* 1993;43:1683–1689.
17. Wardlaw JM, Smith EE, Biessels GJ, et al. Neuroimaging standards for research into small vessel disease and its contribution to ageing and neurodegeneration. *Lancet Neurol* 2013;12:822–838.
18. Jeon S, Yoon U, Park JS, et al. Fully automated pipeline for quantification and localization of white matter hyperintensity in brain magnetic resonance image. *Int J Imaging Syst Technol* 2011;21:193–200.
19. Tzourio-Mazoyer N, Landeau B, Papathanassiou D, et al. Automated anatomical labeling of activations in SPM using a macroscopic anatomical parcellation of the MNI MRI single-subject brain. *Neuroimage* 2002;15:273–289.

20. Collins DL, Neelin P, Peters TM, Evans AC. Automatic 3D intersubject registration of MR volumetric data in standardized Talairach space. *J Comput Assist Tomogr* 1994;18:192–205.
21. Mori S, Crain BJ, Chacko VP, van Zijl PC. Three-dimensional tracking of axonal projections in the brain by magnetic resonance imaging. *Ann Neurol* 1999;45:265–269.
22. Wang R, Beener T, Sorensen AG, Wedeen VJ. Diffusion Toolkit: a software package for diffusion imaging data processing and tractography. *Proc Int Soc Magn Reson Med* 2007;15:3720.
23. Hagmann P, Sporns O, Madan N, et al. White matter maturation reshapes structural connectivity in the late developing human brain. *Proc Natl Acad Sci USA* 2010;107:19067–19072.
24. Reijmer YD, Freeze WM, Leemans A, Biessels GJ; Utrecht Vascular Cognitive Impairment Study Group. The effect of lacunar infarcts on white matter tract integrity. *Stroke* 2013;44:2019–2021.
25. Shu N, Liu Y, Li K, et al. Diffusion tensor tractography reveals disrupted topological efficiency in white matter structural networks in multiple sclerosis. *Cereb Cortex* 2011;21:2565–2577.
26. Rubinov M, Sporns O. Complex network measures of brain connectivity: uses and interpretations. *Neuroimage* 2010;52:1059–1069.
27. Kang Y, Na DL. *Seoul Neuropsychological Screening Battery*. Incheon: Human Brain Research & Consulting; 2003.
28. Ahn HJ, Chin J, Park A, et al. Seoul Neuropsychological Screening Battery–dementia version (SNSB-D): a useful tool for assessing and monitoring cognitive impairments in dementia patients. *J Korean Med Sci* 2010;25:1071–1076.
29. Chao LL, Decarli C, Kriger S, et al. Associations between white matter hyperintensities and beta amyloid on integrity of projection, association, and limbic fiber tracts measured with diffusion tensor MRI. *PLoS One* 2013;8:e65175.
30. Lee DY, Fletcher E, Martinez O, et al. Regional pattern of white matter microstructural changes in normal aging, MCI, and AD. *Neurology* 2009;73:1722–1728.
31. Tullberg M, Fletcher E, DeCarli C, et al. White matter lesions impair frontal lobe function regardless of their location. *Neurology* 2004;63:246–253.
32. Park JH, Seo SW, Kim C, et al. Effects of cerebrovascular disease and amyloid beta burden on cognition in subjects with subcortical vascular cognitive impairment. *Neurobiol Aging* 2014;35:254–260.
33. Cavanna AE, Trimble MR. The precuneus: a review of its functional anatomy and behavioural correlates. *Brain* 2006;129:564–583.
34. Seo SW, Im K, Lee JM, et al. Cortical thickness in single-versus multiple-domain amnesic mild cognitive impairment. *Neuroimage* 2007;36:289–297.
35. Kim J, Kim YH, Lee JH. Hippocampus-precuneus functional connectivity as an early sign of Alzheimer's disease: a preliminary study using structural and functional magnetic resonance imaging data. *Brain Res* 2013;1495:18–29.
36. Kim HJ, Ye BS, Yoon CW, et al. Cortical thickness and hippocampal shape in pure vascular mild cognitive impairment and dementia of subcortical type. *Eur J Neurol* 2014;21:744–751.
37. Du AT, Schuff N, Chao LL, et al. White matter lesions are associated with cortical atrophy more than entorhinal and hippocampal atrophy. *Neurobiol Aging* 2005;26:553–559.
38. Ginsberg SD, Martin LJ. Axonal transection in adult rat brain induces transsynaptic apoptosis and persistent atrophy of target neurons. *J Neurotrauma* 2002;19:99–109.
39. Schallert T, Jones TA, Lindner MD. Multilevel transneuronal degeneration after brain damage: behavioral events and effects of anticonvulsant gamma-aminobutyric acid-related drugs. *Stroke* 1990;21:143–146.
40. Wedeen VJ, Wang RP, Schmahmann JD, et al. Diffusion spectrum magnetic resonance imaging (DSI) tractography of crossing fibers. *Neuroimage* 2008;41:1267–1277.

20 Minutes Pack a Punch

Neurology[®] Podcasts

- Interviews with top experts on new clinical research in neurology
- Editorial comments on selected articles
- Convenient—listen during your commute, at your desk, or even at the gym
- On demand—it's there when you want it
- Fun and engaging
- New topic each week
- FREE

Listen now at www.aan.com/podcast